

# ULTIMATE BEHAVIOR OF HEAVY STEEL SECTION WELDED SPLICES AND DESIGN IMPLICATIONS

By Michel Bruneau,<sup>1</sup> Associate Member, ASCE,  
and Stephen A. Mahin,<sup>2</sup> Member, ASCE

**ABSTRACT:** Full- and partial-penetration butt-welded splices of American Institute of Steel Construction (AISC) group four and five rolled steel sections are tested. Test specimens are devised so splices are located in regions of pure bending. The partial-penetration splice is able to develop and exceed its nominal capacity. However, it fails in a brittle manner with no apparent ductility. Qualitative explanations are given as to the cause of the observed failure. The adequacy of simple strength-design methods to predict that behavior is assessed. Also, an example is presented for braced frames designed according to the Uniform Building Code (UBC). The acceptability of partial-penetration welds in that design is reviewed by comparing the member forces obtained from the static analysis with those resulting from an inelastic step-by-step dynamic analysis. The specimen with a full-penetration welded splice exhibits satisfactory strength and ductility. It is believed, however, that a great amount of care must be taken in the execution of this type of weld. Design implications of those results for seismic resistant structures are examined.

## INTRODUCTION

Structural steel sections in groups four and five are extensively used as compression members in tall buildings and other large structures. The AISC ("Specifications" 1980) currently does not recommend the use of such sections in designs requiring welding or thermal cutting unless the adequacy of material properties for such applications are determined. When these sections are spliced with full-penetration welds and used as members subjected to primary tensile stresses due to tension or flexure, a recent supplement to the AISC ("Specifications" 1989) specifies special Charpy V-notch testing requirements, along with some other weld-preparation requirements. There are, however, numerous applications where the use of such members in tension in the as-received condition with welded joints seems to provide a good design solution.

For example, such sections seem to be a logical choice in long-span space frames and trusses, where architectural and other requirements necessitate large tension chords with small overall dimensions. A more common situation is encountered in the design of tall structures. Columns in these buildings are generally designed to carry compressive loads, and are rarely subjected to net calculated tensile forces. In such situations, group four and five sections may be the logical design choice. For structures located in seismically active regions, however, the lateral forces developed during severe earthquakes can result in large overturning moments, which may in turn induce significant tensile as well as compressive forces in the columns. The design of welded tension connections and tension splices introduces special

<sup>1</sup>Asst. Prof., Dept. of Civ. Engrg., 161 Louis Pasteur, Univ. of Ottawa, Ottawa, Ontario, Canada, K1N 6N5.

<sup>2</sup>Prof., Dept. of Civ. Engrg., Univ. of California, Berkeley, CA 94720.

Note. Discussion open until January 1, 1991. To extend the closing date one month, a written request must be filed with the ASCE Manager of Journals. The manuscript for this paper was submitted for review and possible publication on February 16, 1989. This paper is part of the *Journal of Structural Engineering*, Vol. 116, No. 8, August, 1990. ©ASCE, ISSN 0733-9445/90/0008-2214/\$1.00 + \$.15 per page. Paper No. 24978.

problems when heavy rolled sections are used in such cases. Unless reliable and economical methods for detailing welded tension connections are available, designers may be understandably reluctant to use members fabricated from group four and five sections for these and other similar applications.

In a number of instances, designers have used welded butt splices in tension members fabricated from group four and five sections. Unfortunately, several cases of partial or complete brittle fracture have been reported during fabrication or construction (Bjorhovde 1987; Fisher and Pense 1987; "Welding Manual" 1983; Tuchman 1986). A wide variety of opinions have been expressed about the cause of this unsatisfactory performance. Some have attributed these problems to the microstructural features and segregation (especially in the region contiguous to the flange and web) that occur in such sections because of relatively high alloying, limited rolling, and high finish temperatures employed in their manufacture. Others allege the unsatisfactory performance is a result of inadequate weld design or the use of improper or poorly executed welding procedures. This situation casts considerable uncertainty over the safety and use of these types of members in tension.

This paper presents the results of a testing program of partial- and full-penetration butt-weld splices of typical group four and five sections, as presently fabricated by industry, and examines some analytical results to assess the practical design implications of the observed behavior. A more detailed discussion of the various factors contributing to produce the behaviors observed may be found in Bruneau et al. (1987). This paper emphasizes the practical consequences of the experimentally obtained results.

## **SURVEY OF AVAILABLE DATA**

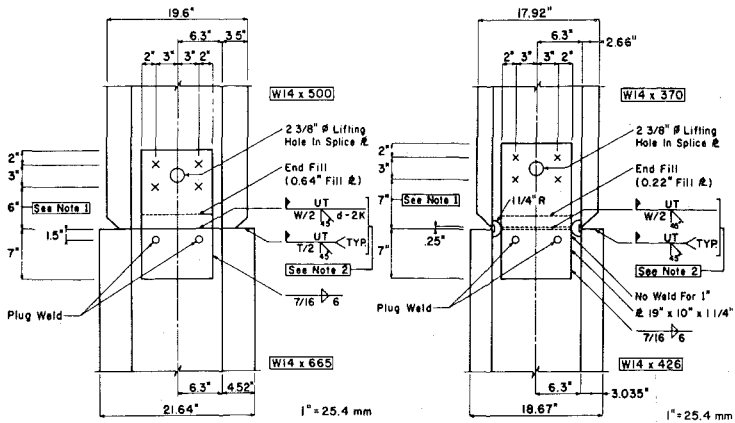
There are several papers in the literature about welding of thick plates, welding-related problems, and general fabrication techniques to be used to minimize the occurrence of these problems. However, nearly all this information is of a qualitative nature ("Commentary" 1973; Blodgett 1977; Blodgett 1979; Doty 1987; Kaufmann and Stout 1983; Preece 1981; Yurioka et al. 1983). Relatively little quantitative information is available related to the field performance and experimental behavior of tension splices in heavy section members.

Detailed published reports of the findings of structural failure investigations are few (Bjorhovde 1987; Fisher and Pense 1987; Tushman 1986). Nevertheless, some prominent cases have been reported (e.g., Fisher and Pense 1987), for which high residual stresses and particularly low notch toughness of the base material are said to be responsible for failure at the joints.

Some tests of partial- and full-penetration tension splices in group four sections have been reported (Popov and Stephen 1976). These specimens were tested in pure tension, but only the flanges were welded. Thus, these specimens avoided the high residual stress conditions induced by the welding of the webs and present in the observed field failures. These test specimens were able to develop their calculated capacities, but, in general, most sections exhibited very little ductility.

## **TEST SPECIMEN CONFIGURATION**

Because of the aforementioned lack of quantitative data regarding the mechanical behavior of splices in group four and five sections, a series of ex-



**NOTES:**

1. Provide 6" *as specified* instead of 3" as on standard detail.
2. A certified inspector is to be present during construction and perform ultrasonic testing of the weld.

**NOTES:**

1. Provide 7" *as specified* instead of 3" as on standard detail.
2. A certified inspector is to be present during construction and perform ultrasonic testing of the weld.

**FIG. 1. Test Specimens: (a) Partial-Penetration Welded Splice Detail; (b) Full-Penetration Welded Splice Detail**

perimental and analytical studies were undertaken. At the recommendation of an advisory panel, splice configurations considered were taken to be representative of those used in columns of buildings in seismically active regions. Because full-penetration weldments have suffered the most field difficulties, they were the initial focus of these investigations. However, partial-penetration splices were investigated because they represent the substantial majority of all welds used for column splices. Because failures have been observed primarily in high-strength A572 grade 50 steel weldments, specimens for these experiments were fabricated from that steel. Standard A572 grade 50 steel is not only believed to be more widely used, but has a lower notch toughness than A36 grade steel, which makes it more susceptible to brittle failure from a fracture-mechanics point of view. Special attention was placed on making the specimens representative of current engineering and fabrication practices. In these investigations, no efforts were made to modify the metallurgical properties of the base metal or to develop special-purpose weld procedures.

A partial-penetration weld of 50% of the flanges ( $t/2$ ) and 50% of the web ( $w/2$ ) is often specified by engineers in seismic regions [Fig. 1(a)]. It also corresponds to a minimum weld detail for some codes in specific circumstances. For example, the *Uniform Building Code* (1988) requires this for trusses (Sec. 2712g), and the Structural Engineers Association of California's "Recommended Lateral Force Requirements and Commentary" (1988) stipulates it for columns when there is any net calculable tensile force (Commentary Section 4-d). When full-penetration welds are specified for building columns, they are often detailed for construction reasons with the flanges completely welded ( $t$ ) and the web partially welded ( $w/2$ ) [Fig. 1(b)]. Therefore, a partial-penetration connection and a full penetration one, as shown on Figs. 1(a) and (b), were selected for testing. The splice design details



The splice area was preheated to 250° F (121° C) and the interpass temperature was controlled during execution of the weld. The fabricator judged the ambient temperature (about 70° F, or 21° C) to be sufficiently warm so the specimen could be air cooled. Visual inspection and ultrasonic inspection of the base metal and weld were executed, and no defects were reported.

### **Specimen Two—Full-Penetration Weld**

The second specimen was a full-penetration butt weld connecting a W14 × 370 to a W14 × 426. These were practically the largest sizes that could be accommodated on the testing machine with a full-penetration splice.

The copes at the web-flange intersection were ground smooth, as was the custom with the fabricator. This provided a smooth surface in the critical intersection zone of the metal where the metallurgy is of inferior quality. In previously reported failure case studies (Tuchman 1986), flame-cut copes created a very jagged and brittle martensite surface that served as crack initiators. The grinding of these flame-cut cope holes should be noted when interpreting the test results. Another special feature was the root pass for the flange welds, which was located in the back-up bars.

The specimen was preheated to 250° F (121° C). Interpass temperature was controlled. E70-311 low hydrogen electrodes were used. After completion of the weld, the splice area was wrapped with a thermal blanket to help slow cooling overnight. Ambient temperatures at the time of welding were estimated to be 60–70° F (15–21° C). Ultrasonic inspection of the base metal and weld revealed no defects.

## **SPLICE WITH PARTIAL-PENETRATION WELDS**

### **Description of Testing**

The partial-penetration weld is obviously the weakest link along this specimen, as it is expected to transfer only about half the capacity of the smaller of the two sections connected to it. Any yielding in this first specimen was expected, therefore, to be concentrated in the steel immediately adjacent to the weld area, since the yield stress of steel is presumably lower than that of the weld material.

Because of this, an *X-Y* plot of the moment-curvature relationship [as measured by clip-gauges on a 6-3/4 in. (171 mm) gauge length] at the center splice was used to monitor the behavior of the splice as the loading program progressed. Two other pairs of clip gauges were installed on each side of the central pair to allow curvatures to be deduced for the regions near the splice. Although 29 channels of data were recorded for subsequent evaluation, only the clip-gauge results will be presented in this paper. All data were recorded by a microcomputer-based data acquisition system.

The first step in the loading program was to slowly, gradually load the specimen through the elastic design range to its yield capacity, as evidenced by a small plastic offset in the moment-curvature plot. After this point the specimen was to be unloaded and inverted for subsequent cyclic loading. Applied loads during the first step exceeded those corresponding to theoretical values of  $M_y/2$  and  $M_p/2$  for the smaller section, assuming a nominal yield stress of 50 ksi (345 MPa). Since the moment-curvature plot was still linear, loading was continued without apparent distress or yielding up to the theoretical fully plastic state of a fictitious steel cross section created by the

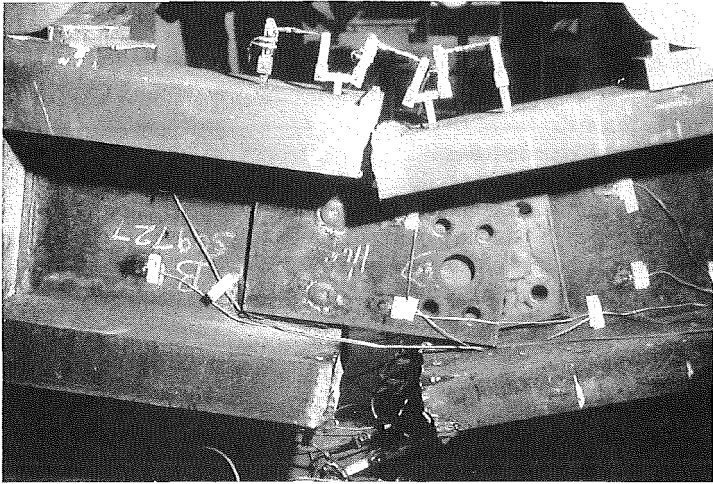
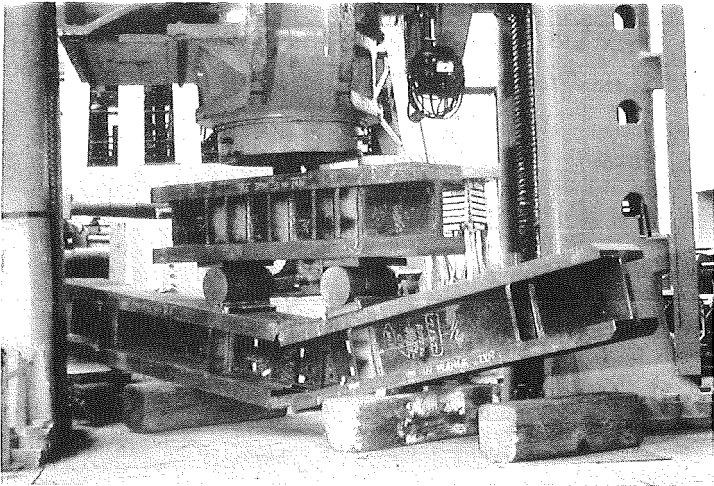


**FIG. 3. Failure of Partial-Penetration Welded Splice: (a) Global Specimen Failure; (b) Close-up of Failed Splice**

welded surfaces. Following a 30 sec pause to visually inspect the specimen and the measurements, loading was increased to detect initial yielding. The moment-curvature relationship remained practically linear to a moment of approximately 35,400 kips-in. (4,000 kN-m) [last digitized value is 34,992 kips-in. (3,954 kN-m)] when a sudden and brittle failure occurred across the entire section through the weld [Figs. 3(a) and 3(b)].

Once failure started in the tension (bottom) flange, the part of the section remaining intact was unable to accommodate the imposed displacement. The failure then quickly progressed through the whole section. The erection plate did not appear to restrain or stabilize the failure once it initiated. The errec-

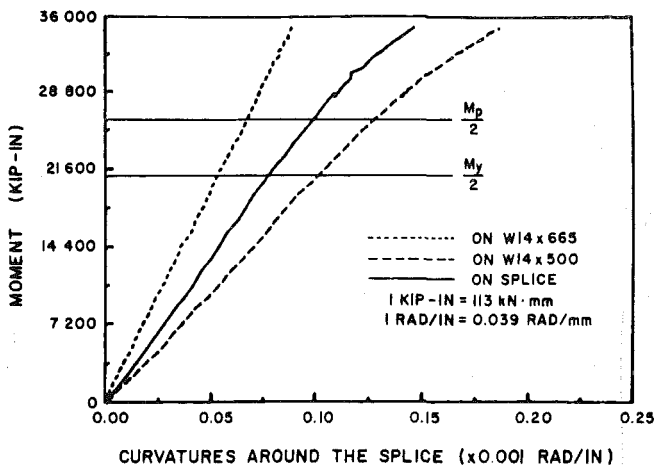


FIG. 4. Moment-Curvature Relationship from Clip Gauges for Partial-Penetration Specimen

tion bolts were sheared suddenly and thrown with considerable energy away from the splice. Temperature at time of testing was around 55° F (13° C).

#### Experimentally Recorded Results

Detailed description of the failure surface, estimates of stress-intensity factor  $K_I$  at failure, and presentation of all recorded information during testing are beyond the scope of this paper and presented elsewhere (Bruneau et al. 1987). It is nevertheless noteworthy that inspection of the failure surface (A. Collins, welding consultant, private communication, 1985) indicated a lack of fusion between some weld passes, and a lack of penetration and fusion of the root passes. Nonetheless, it is believed that even a better weld would have fractured in a brittle mode.

From the recorded data, the most meaningful information, shown on Fig. 4, was provided by three pairs of clip gauges with gauge lengths of approximately 6 in. These clip gauges measured global yielding effects in the splice area. The moment-curvature relationship derived from the clip gauges on the W14 × 665 remains perfectly elastic, and is almost identical to the theoretical one. As the moments get above 28,800 kips-in. (3,254 kN-m), a slight softening of the moment-curvature relation can be observed for the other two regions. Local yielding due to residual stresses is likely the cause of the softening observed for the W14 × 500. However, at failure, none of the measured curvatures exceeded the predicted elastic values by more than 10%.

#### Analysis of Probable Stresses at Failure

Stresses can be estimated from the observed data in a few different ways. The fact that linearity was preponderant during the test permits the use of some simplifying assumptions. For example, estimates of maximum stresses at cross sections away from the splice on the partial-penetration specimen can be obtained from the strains measured and by assuming linear-elastic

behavior. The maximum stresses thus obtained at the time of failure were 30.8 ksi (212 MPa) and 42.3 ksi (292 MPa) on the W14 × 665 and W14 × 500 sections, respectively. These stresses do not exceed the nominal yield value for sections away from the splice.

This approach is, of course, inaccurate near the weld since it completely neglects the stress-concentration factor created by the partial penetration, as well as the initial residual stresses. Nonetheless, it is interesting to estimate the strength of the splice as one might do in design. Plane sections are assumed to remain plane, and either linear-elastic or simple plastic material properties are used. For these estimates, the material is assumed to yield at 50 ksi (345 MPa). If one estimated the capacity of the splice by taking one-half of the yield capacity ( $M_y$ ) of the smaller section, the experimentally measured capacity is 59% greater. The measured capacity is also 35% greater than  $M_p/2$  of the smaller section. A more detailed analysis based on the full plastic-moment capacity of the welded portions of the smaller section results in an estimate 20% less than the measured capacity. Thus, the section strength is conservatively estimated by standard methods.

Stresses also can be computed using such methods at the observed failure section. This can have a significant effect here because of the large difference in flange thicknesses between the two sections. Should the smoothed weld transition as used on the specimen be included in the calculations, the stresses computed again using simplified elastic analysis methods at various potential failure surface sections are significantly lower than the nominal yield value, ranging from 43–45 ksi (296–310 MPa), depending on the selected critical surface, or approximately 90% of the nominal yield capacity. This implies that these critical sections would have remained elastic at failure. Obviously, all these methods neglect the very important effects of stress concentration and residual stresses. However, the thickening of the section due to the transition welds provides one reason for the apparent high capacity of the splice.

To gain a qualitative understanding of the stresses near the splice at the time of failure, elastic finite element procedures can be used. The presence of discontinuities in the mesh makes the results inexact, but it allows one to gain a feeling for the stress distribution across the depth of the section near the weld. To estimate the true stresses at the tip of the crack, a very fine mesh would be required in that critical zone and a more refined material model would also be needed, considering nonlinearity and fracture. Fracture mechanics methods could serve the same purpose. In this analysis, the tension flange is modeled as a plane strain slice continuously supported at the web-flange location. The two-dimensional model neither reflects the variations induced by shear lag, nor accounts for residual stresses.

Results for a model (Fig. 5) where a progressive change of thickness is introduced, as expected in a properly executed weld, are presented here. Other models were investigated elsewhere (Bruneau et al. 1987) to assess the effect of different transition configurations. Smoothing the weld does not change the basic nature of the results, but helps reduce the overall stresses and discontinuity effects.

Loads (stresses) were imposed to approximate the states of stress in the flanges away from the splice at the time of failure. Results obtained are summarized on Fig. 5, and emphasize the fact that, while uniform varying stresses would be expected away from the weld, very high stresses would

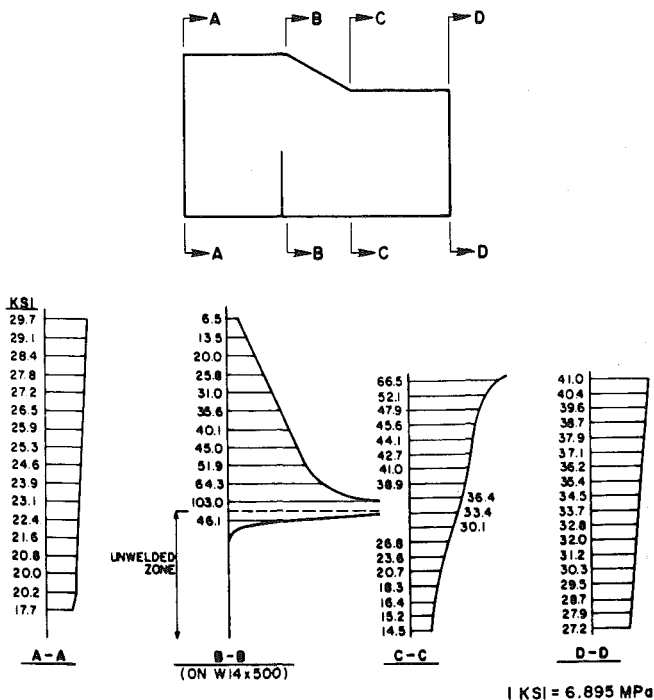


FIG. 5.  $\sigma_{11}$  Stress Magnitudes and Distribution Profile for Finite Element Analysis Results along Selected Cross Sections

concentrate at the tip of the crack. Stresses much higher than yield are predicted, thereby violating the assumptions in the analyses.

The finite element results clearly reveal the stress-concentration effect produced by the unwelded half of the flange. It effectively acts like an initial crack. The maximum stresses occur near the root of the weld, not at the top where they are predicted to occur by traditional methods of calculation.

Although the previous discussion mainly emphasized the presence of excessive stress concentration in the flange due to the cracklike effect of the unwelded part of the flange, it must be realized that the brittle failure was apparently a result of a combination of factors. As discussed by Bruneau et al. (1987), other significant factors include bad fusion of the weld passes, critical weld configuration, and low effective gauge length around the weld.

The design capacity of the section has been significantly exceeded. Nevertheless, this failure is rather disconcerting as it occurs in the weld suddenly, without warning. Moreover, conventional design methods not based on fracture mechanics ignore the cracklike discontinuity inherent in partial-penetration welds when assessing local stresses.

### Some Design Implications for Seismic Resistant Braced Frames

Partial-penetration column splices, such as those tested here, are mandated by several codes (*Uniform* 1988) for structures in seismic zones when any net tensile load is computed. Using conventional allowable-stresses design

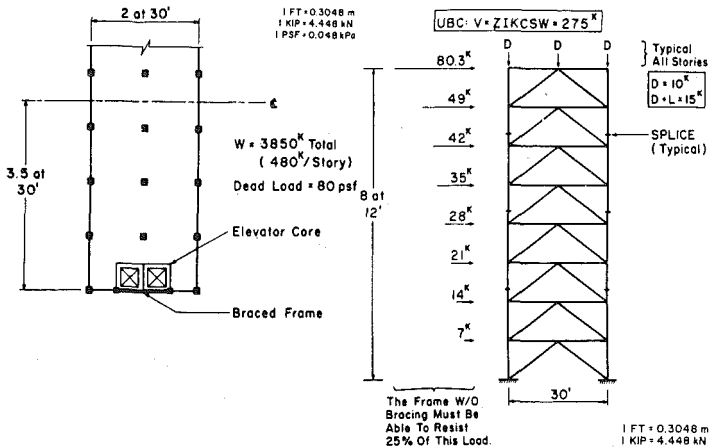


FIG. 6. Braced-Frame System Designed by the Uniform Building Code: (a) Floor Plan; (b) Geometry, Splice Location, and Applied Forces

methods, it is possible to design such a building in the belief these column splices would not be subjected to tensile loads greater than  $P_y/2$  or to moments greater than  $M_p/2$ . In such cases, half-penetration welds may provide a functional and economical design solution. However, actual earthquake-induced actions can exceed these values in certain cases.

To illustrate this, an eight-story braced frame was designed using the 1985 edition of the *Uniform Building Code* (Uniform 1985). The geometry of the structure and the resulting design are shown in Figs. 6(a) and 6(b). No efforts were made to obtain large sections similar to the ones tested during this investigation ( $W14 \times 665$  and  $W14 \times 500$ ), but this could have been

TABLE 1. Eight-Story Braced Frame: UBC Analysis<sup>a</sup>

Story (1)	MAXIMUM FORCES FROM UBC ANALYSIS				ALLOWABLE FORCES		
	Columns		Braces		Column	Splice	Brace
	Compression (2)	Tension (3)	Compression (4)	Tension (5)	Compression (6)	Tension (7)	Compression (8)
1	-713	426	-186	164	-701	—	-241
2	-582	333	-185	162	-701	—	-241
3	-457	245	-176	154	-472	286	-241
4	-341	166	-162	141	-472	—	-241
5	-236	98	-145	123	-237	177	-146
6	-144	44	-122	101	-237	—	-129
7	-70	7	-95	75	-237	177	-114
8	-15	—	-63	43	-237	—	-63

<sup>a</sup>Component dimensions: Columns, first and second stories,  $W12 \times 96$ ; third and fourth stories,  $W12 \times 65$ ; fifth through eighth stories,  $W12 \times 40$ . Beams, first and second stories,  $W12 \times 106$ ; third and fourth stories,  $W12 \times 96$ ; fifth story,  $W12 \times 87$ ; sixth story,  $W12 \times 79$ ; seventh and eighth stories,  $W12 \times 45$ . Braces, first through fourth stories,  $W12 \times 53$ ; fifth story,  $W12 \times 50$ ; sixth story,  $W12 \times 45$ ; seventh and eighth stories,  $W12 \times 40$ . Column splices occur at the third, fifth, and seventh stories.

done simply by changing the floor plan and building height. In this design, W12-compact sections were used for all structural members (Table 1) to facilitate detailing of the connections.

The floor plan considered in this example transfers very little of the dead and live loads to the columns of the braced frame, especially compared to the axial forces due to the lateral equivalent force calculated by the *Uniform Building Code* (UBC). Dead loads on the braced bent were 30 kips (133 kN) per story, and live loads were 15 kips (67 kN) per story, distributed as shown in Fig. 6(b). The UBC seismic forces were obtained using the following equation.

$$V = ZIKCSW \dots\dots\dots (1)$$

in which  $Z = 1.0$ ;  $I = 1.0$ ;  $K = 0.8$ ;  $S = 1.5$ ;  $C = 1/15(T)^{0.5}$ ; and  $W = 3,850$  kips (17,125 kN). As a result,  $V = 275$  kips (1,223 kN).

The resulting load distribution is shown in Fig. 6(b). The period  $T$  of the structure was computed to be 1.25 sec after a few design iterations. The frame design satisfies all of the UBC strength and stiffness requirements. The 1.25 load increase factor prescribed for braced frames and the 1.33 increase in allowable stress permitted in seismic design have both been conservatively omitted in this example since they practically cancel. The bare frame (without bracing) is able to resist 25% of the loads applied, as required for the use of a  $K$  factor of 0.8. Resulting member design axial forces are shown in Table 1. Note that maximum compression and tension forces resulted from different load cases.

All splices were located in regions where the maximum calculated tension force (from UBC analysis) was less than one-half of the allowable tension load of the smaller section at the splice. Moments at splice locations were negligible. Therefore, a designer might use partial-penetration butt welds for the column splices.

Several inelastic dynamic analyses of this frame were performed. Stiffness-proportional viscous damping was chosen, with 2% of critical damping provided at the first mode period, the post-yield strain-hardening ratio for the members was taken as 0.05, and the yield stress was assumed to be 50 ksi (345 MPa). In the example presented here, buckling of the braces also occurred at 50 ksi (345 MPa), corresponding to very stocky braces. Results for more slender braces are presented elsewhere (Bruneau et al. 1987). The unscaled  $N-S$  component of the 1940 El Centro earthquake was used as the input for the system (0.34g peak acceleration). To illustrate the critical condition for the splices, no live loads were included in this analysis, and only 80% of the design dead load was considered simultaneously with the earthquake. For these analyses, the splices were assumed to be able to transfer the full capacity of the members connected, and failures in the splices of columns were not modeled in the analysis.

Time histories of the axial loads at the third- and fifth-floor splices are plotted in Fig. 7. These splices reached their failure loads nearly simultaneously; at only 1.96 sec after initiation of earthquake motion. Numerical values for the resulting demands are presented in Table 2. Failure of the splices was defined here to occur when an axial load developed equal to  $P_y/2$  of the smaller section at the splice. In light of the results of the testing program, it could have been increased slightly, delaying the failure by a fraction of a second. The rest of the column response in Fig. 7 shows these

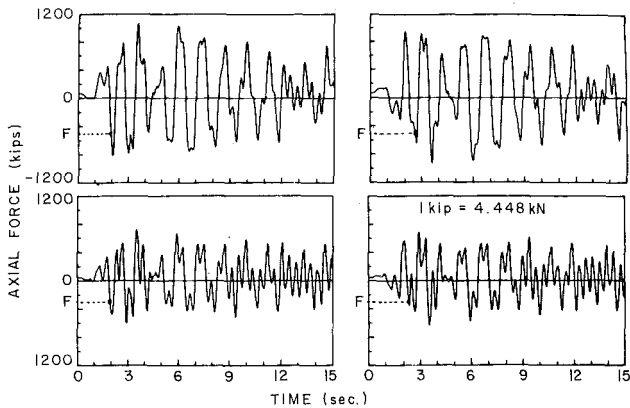


**FIG. 7. Time History of Axial Force in Third-Story Splice (Top Graphs) and Fifth-Story Splice (Bottom Graphs)—Left and Right Columns ( $F$  = Predicted Failure Force Level)**

large axial tensile forces are demanded many times. The gravity loads in the columns (see time zero in Fig. 7) are very low compared to the fluctuations associated with the dynamic excitation. Consequently, it is important to note that even if full dead and live load were used, the same results would occur with the initial failure slightly delayed.

Analyses were also performed using more slender braces with a critical buckling stress of 25 ksi (172 MPa). These additional analyses produced similar results with larger inelastic demands on the columns, coupled with large inelastic demands on the bracing system. Failure of the splices occurred

**TABLE 2. Eight-Story Braced Frame: Nonlinear Analysis<sup>a</sup>**

Story (1)	MAXIMUM FORCES FROM NONLINEAR ANALYSIS				$P_y/2$ of smallest section at splice (6)
	Columns		Braces		
	Compression (2)	Tension (3)	Compression (4)	Tension (5)	
1	-1,709	1,529 <sup>b</sup>	-787	784 <sup>b</sup>	—
2	-1,319	1,161	-780	778	—
3	-1,068	931 <sup>b</sup>	-637	624	478
4	-907	796	-509	494	—
5	-724	635 <sup>b</sup>	-429	414	295
6	-522	459	-372	361	—
7	-298	258	-370	357	295
8	-89	73	-253	241	—

<sup>a</sup>Component dimensions: Columns, first and second stories, W12 × 96; third and fourth stories, W12 × 65; fifth through eighth stories, W12 × 40. Beams, first and second stories, W12 × 106; third and fourth stories, W12 × 96; fifth story W12 × 87; sixth story, W12 × 79; seventh and eighth stories, W12 × 45. Braces, first through fourth stories, W12 × 53; fifth story, W12 × 50; sixth story, W12 × 45; seventh and eighth stories, W12 × 40. Column splices occur at the third, fifth, and seventh stories.

<sup>b</sup>Members responded inelastically (yielded).

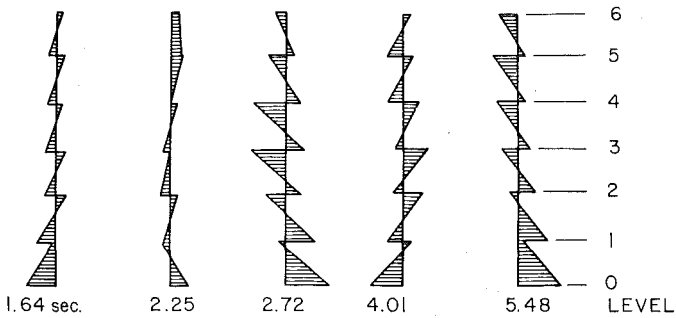


**FIG. 8. Movement of Inflexion Point in Columns of Moment Frame Responding Nonlinearly to El Centro Earthquake 1940 *N-S* Component (From Park and Pauley 1975)**

slightly sooner, as it would have had the intensity of the earthquake been increased.

If the 1988 *Uniform Building Code* (1988) were followed in the design instead of the 1985 edition, it would result in a reduction of approximately 10% in the lateral force requirement level. However, the new code stipulates that partial-penetration column splices be designed for the 150% of the axial load required in the column. This design load is based on  $1.0P_D + 0.7P_L + (3/8)R_W P_E$  for compression and  $0.85P_D + (3/8)R_W P_E$  for tension, where  $P_D$ ,  $P_L$ , and  $P_E$  are the loads due to dead, live, and earthquake loading, respectively, and  $R_W$  is a response modification factor equal to 10 in this case. This amplification of seismic forces and the requirement of 150% overstrength for partial-penetration welds substantially increase column-size requirements and virtually eliminate the use of partial-penetration welds for this structure.

### Some Implications for Seismic Resistant Moment Frames

Similar problems with partial-penetration butt-welded splices may also occur in ductile moment-resisting frames. Splices are usually located in the middle third of a column, where moments are presumed to be small. Nonlinear dynamic analyses indicate this assumption is not always valid, and the point of inflection may move for from midheight of the column. For example, Park and Pauley (1975) commented about the discrepancies between the distributions of bending moment obtained from static lateral loading and those that might occur in columns of multistory frames as a result of severe dynamic excitations. Nonlinear analysis reveals "that at certain times during the response of the structure to earthquake ground motions, the point of contraflexure in a column between floors may be close to the beam-column joint and the column may even be in single curvature at times. The reason for the unexpected distribution of column bending moments at some instants of time is the strong influence of the higher modes of vibration, particularly the second and third modes." This is illustrated in Fig. 8.

Even for static code lateral loads there may not be any points of contraflexure for some stories. Plastic moment redistribution may also result in significant shifts of the point of inflection. Failure to design for realistic estimates of seismic stresses at the splice may result in overstress and brittle

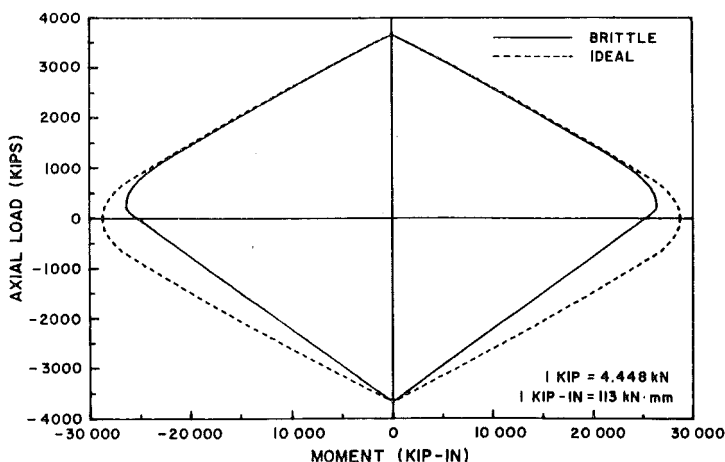


**FIG. 9. Moment-Axial Load Interaction Diagram for Theoretical Partial-Penetration Cross Section Under Idealized Linear Strain Distribution and Brittle Failure at 50 ksi**

failure of welded partial-penetration splices in heavy sections. This behavior is further complicated if biaxial bending effects are considered.

#### **Effect of Axial Force on Behavior**

It should be recognized that most columns in buildings will be subjected to net compressive loads in addition to bending. In such cases, the compression flange will begin yielding prior to fracture of the tension flange. Thus, some ductility may be exhibited by these connections. However, if the rotation demand becomes large, the column will still fracture. Precise computation of the moment-axial load-ductility interaction of such splices is difficult, but preliminary evaluations are possible using simple assumptions.

For example, an interaction diagram can be derived for a connection whose capacity is limited by brittleness of the tension flange. The material is modeled as linear elastic and perfectly plastic in compression, and elastic and brittle in tension. Plane sections are assumed to remain plane. The footprint of the nominal welded area ( $t/2$  and  $w/2$ ) constitutes the chosen effective cross section, as could be done in design. Consequently, unwelded portions are assumed not to contribute to the compression resistance of the section. The smaller section joined in the partial-penetration splice specimen is used as the basis for dimensions in this example. Failure is defined to occur when tension exceeds 50 ksi (345 MPa) at any point in the section. The resulting axial load-bending moment ( $P$ - $M$ ) interaction curve is presented in Fig. 9. This  $P$ - $M$  interaction surface is equivalent to one obtained using linear-elastic analysis methods when the axial force is tensile. However, under a compression force, it falls somewhere between curves obtained using linear-elastic and perfectly plastic material assumptions.

Furthermore, the moment-curvature relationship can be drawn for various levels of compressive forces (Fig. 10). The curvature ductility, nonexistent in absence of axial compression, increases to more than 10 when 2,000 kips

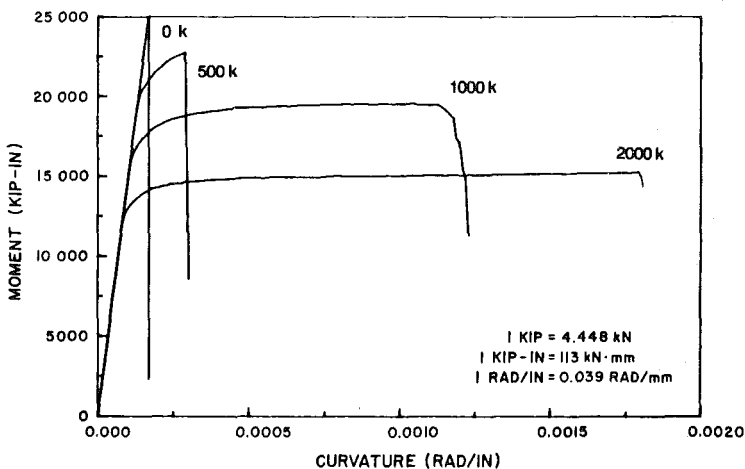


**FIG. 10. Moment-Curvature Curves for Theoretical Partial-Penetration Cross Section under Idealized Linear Strain Distribution and Brittle Failure at 50 ksi**

(8,896 kN) is applied axially. Consequently, some ductility can be obtained with these splices if columns always remain under large compressive forces. Unfortunately, the magnitude of the axial compression force in columns during severe seismic excitations is uncertain.

## **SPLICE WITH FULL-PENETRATION WELDS**

### **Description of Testing**

The full-penetration weld specimen consisted of a W14 × 370 section connected to a W14 × 426 section, as described previously. As for the previous specimen, pairs of clip gauges were installed across and next to the weld, but this time two X-Y plots of the moment-curvature relationships were used to monitor the behavior of the specimen as the loading program progressed, since significant yielding could now occur in both the smaller section (W14 × 370) and the splice area. The specimen was instrumented with a total of 35 channels of data recorded for evaluation. Only the clip gauge results will be presented in this paper.

The loading sequence is schematically illustrated in Fig. 11. Rather than simply loading the specimen monotonically to a target displacement value, as done for specimen one, numerous load excursions were employed in each direction before load reversal. By these successive loadings and unloadings to progressively larger force levels, the resiliency and deterioration of the specimen could be measured. More than 24 load excursions were applied during one complete cycle of deformation reversal.

The specimen was coated with a brittle white paint, and, therefore, inelastic regions were easy to identify as yielding produced cracks in the paint. Some yield (Ludde's) lines were locally observed at midwidth on the outer face of the tension flange of the W14 × 370 near the weld as soon as 60% of the nominal yield level was approached. More of those lines appeared as loading progressed slightly beyond the nominal yield level. No yield lines

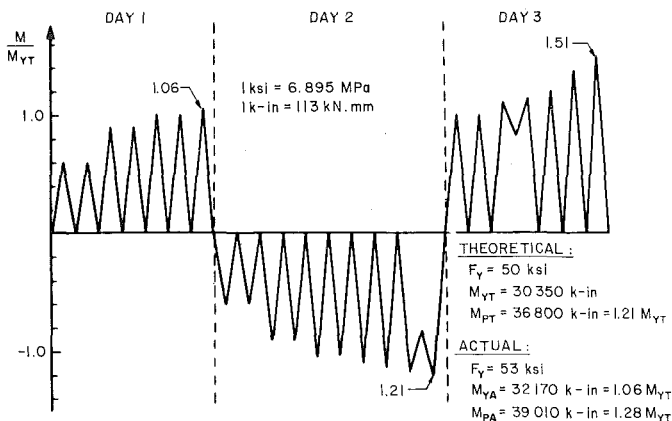


FIG. 11. History of Loading Applied to Full-Penetration Specimen

were observed on the compression flange in this first stage of the experiment. Large residual stresses were believed responsible for this early non-linearity. The initial distribution of residual stresses associated with rolling is significantly altered by the welding process. Since the web was completely welded first, the weld shrinkage in the flanges induced additional tension residual stresses in the flanges. This resulted in a nonsymmetrical stress distribution in the section under the applied loading, causing the tension flange to yield first.

The specimen was then inverted and a similar loading history was applied. After the nominal  $M_y$  level was reached, curvatures were used to control the testing progress. The curvatures obtained in the first part of testing were matched in this part of the test, and then increased until the nominal value of  $M_p$  was reached. Yield lines also became apparent during this loading at the web-flange intersection and all through the tension flange, and compression yield lines (buckled paint) were visible on the inside of the compression flange.

To complete the displacement cycle, the specimen was again inverted, loaded directly to yield, then subjected to progressively larger curvature excursions. More yield lines propagated in both flanges and in the web of both sections. The member was loaded, until a deflection of 2.4 in. (61 mm), or 1.5% of its span, was measured at the splice location, to simulate interstory drifts that might be anticipated during major earthquakes. The moment required to reach that state was 25% greater than the nominal value of  $M_p$ . Note that  $M_p$  is 21% more than  $M_y$  for this section. These moments were large enough to induce significant yielding in the W14  $\times$  426.

### Analysis of Results

The specimen behaved excellently and the various instruments located on the specimen all recorded regular, full hysteresis loops. No deterioration in properties from excursion to excursion was noticed. The weld behaved very well and was undamaged.

Moment-curvature relationships as deduced from the clip gauges are presented in Fig. 12. From the recorded results, it appears that significant non-

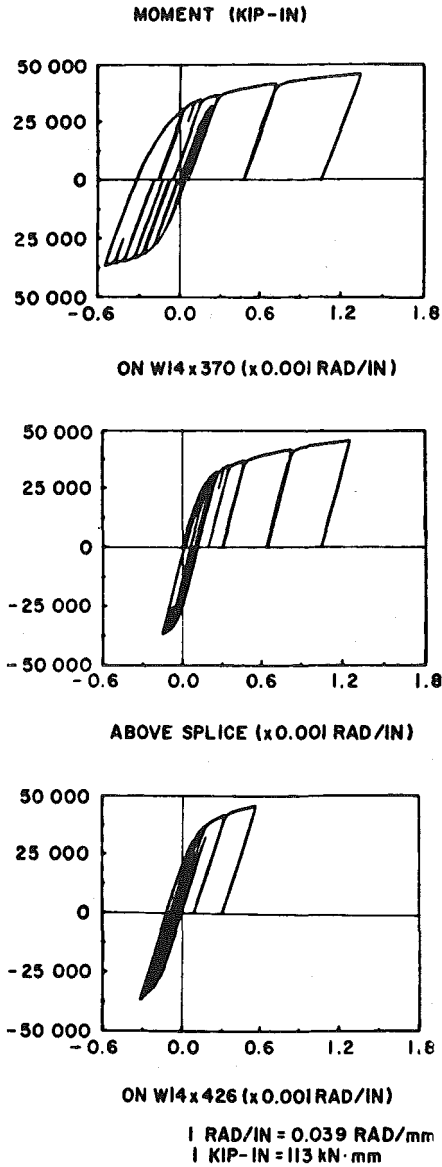


**FIG. 12. Moment-Curvature Relationship from Clip Gauges for Full-Penetration Specimen**

linearity occurred very early, as soon as 40% of nominal  $M_y$  in the splice and 60% of the nominal  $M_y$  in the W14  $\times$  370. Since the clip gauges set across the weld also span some distance along the flange of the W14  $\times$  370, yielding is inferred to have started very close to the weld where the tension residual stresses induced by weld shrinkage were probably the greatest. As

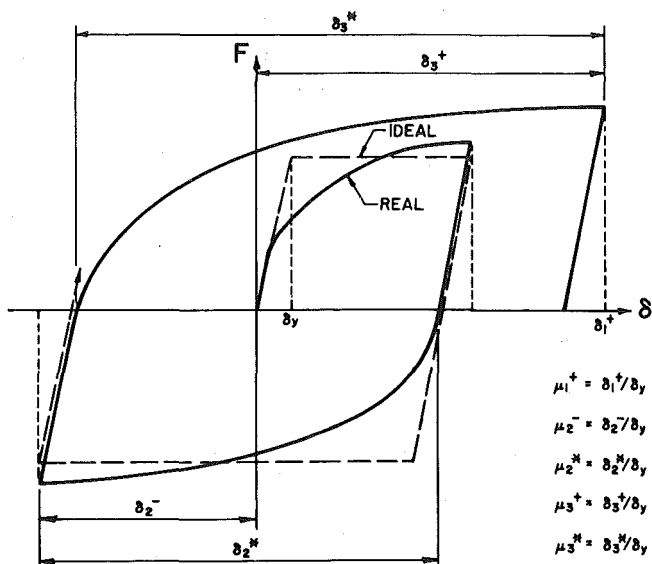


FIG. 13. Ductility Definitions Used

loading progressed, the clip gauges above the W14 × 370 section yielded more than any other, in part because of the strain hardening of previously yielded material immediately adjacent to the weld. In the end, even the W14 × 426 section sustained significant plastic strains as a result of full plastification and strain hardening in the smaller section.

### Ductilities Recorded

It is helpful to make use of a ductility-ratio concept to quantify the contribution of each section to the energy dissipation of the specimen. Since the loading history contains only one complete hysteresis loop, and since the specimen was not tested to failure, it is justified to use only the most elementary definitions of ductility ratio for this study. Fig. 13 illustrates how ductility was defined herein (Mahin and Bertero 1976). Basically, the measured curvature response is divided by the theoretical value corresponding to elastic behavior up to the nominal plastic moment ( $M_p$ ) capacity. Some judgment must clearly be used in interpreting the results. For example, a ductility ratio of less than one does not necessarily mean behavior is still

TABLE 3. Ductilities Measured by Clip Gauges for Specimen No. 2

Gauge location (1)	$\mu_1^+$ (2)	$\mu_2^-$ (3)	$\mu_2^H$ (4)	$\mu_3^+$ (5)	$\mu_3^H$ (6)
W14 × 370	1.07	2.43	2.62	5.97	7.39
Splice	1.16	0.68	1.18	5.66	5.60
W14 × 426	0.83	1.44	1.45	2.62	3.13

linear elastic, since residual stresses initiate nonlinearity at relatively low load levels. Moreover, since  $M_p$  is 21% greater than  $M_y$ , nonlinear behavior is guaranteed to occur before a ductility ratio of one is obtained. A ductility ratio of one could have been defined to occur just at the onset of yielding (and resulting ductilities would have been larger than reported here). Measured ductilities defined in Fig. 13 are tabulated in Table 3. Final curvature-ductility ratio on the W14  $\times$  370 was approximately six. The curvature-ductility ratio developed over the splice region was only slightly smaller.

## SUMMARY AND CONCLUSIONS

### Partial-Penetration Specimen

This test has demonstrated that a partial- (half-) penetration butt weld connecting two heavy jumbo steel sections can develop the design capacity of the connection. The capacity of the splice was more than 25% greater than predicted based on the effective dimensions of the smaller member. This appears in part to be a result of the enlarged weld surface used to make smooth transition between the smaller and larger sections at the splice. Using simple design calculations, however, the apparent maximum stress at the failure surface was less than 90% of the nominal yield capacity of the material. The implications of this for other weld configurations must be carefully assessed.

The splice failed in a very brittle manner when tested under pure bending. The unwelded part of the flange acted like an initial crack, which created a severe stress concentration, accounting for the brittle failure. The poor fusion of the weld passes, the critical weld configuration, the size and poor metallurgical properties of the welded sections, and the low effective gauge length around the weld also contributed to this undesirable failure mode. Continuous visual inspection during welding and ultrasonic testing of the base metal and welds were not sufficient to ensure ductile behavior.

Because of the predominant influence of brittle fracture on the observed mode of failure, a significant size effect must be considered when evaluating such splices. However, it is not known at this stage if all partial-penetration butt welds will behave similarly irrespective of the welded specimen thickness or the degree of penetration. This test and previous research on group four and five steel sections (as well as simple fracture theory) imply the risk of brittle failure is increased with thicker steel.

Designers should be aware of the potential adverse behavior of this detail, and only use it in circumstances where it will not be a structural weak link. This may necessitate evaluation of the inelastic deformation mechanism for the structure. This may be estimated using simple capacity design concepts (Park and Pauley 1975) or an ultimate load analysis for various loading conditions. Designers should also be aware that, in the event of a column-splice failure with net tensile uplift forces, conventional erection plate details may be insufficient to guide the column back to its original position. When these splices are used in locations that might be susceptible to overstressing, alternate details consisting of double-web shear plates (or channels) could be used to prevent misalignment in the event of fracture. However, the adequacy of the details for these connections is as yet unverified.

Additional experimental research is needed to identify the size effect, the performance of joints with small nonpenetrated regions, the influence of ax-

ial loads, and the efficacy of details to prevent misalignment of fractured splices. Analytical and experimental studies are needed to devise practicable and reliable design guidelines for locating and sizing splices in braced and moment frames.

### **Full-Penetration Specimen**

Plasticity apparently started near the weld on the  $W14 \times 370$  and progressed quickly along the whole segment of  $W14 \times 370$  under uniform moment. This is a very desirable behavior that protects the weld from excessive straining.

Large residual stresses initially present in the specimen are responsible for the early nonlinearity recorded, occurring at less than half  $M_y$  in some locations. Although residual stresses do not impair the bending capacity of the section, this stiffness softening can be of great consequence. This is especially true if the axial load is large since the buckling capacity is directly proportional to the section's tangent stiffness.

Good ductility is very important for seismic resistant design and it is fortunate that this type of butt weld, when properly executed, behaved in a very ductile manner. Nevertheless, one must recognize this research program originated partly because full-penetration butt welds of AISC group four and five rolled sections have reportedly failed in a brittle manner under very low loads. This test has not simulated the previously reported failure mode, but showed instead that, with proper care, a full-penetration butt weld on very thick, rolled steel sections can have satisfactory behavior.

Therefore, despite the metallurgical and welding problems discussed earlier, it seems these sections can be fully welded and will still perform well if the engineer and fabricator take the necessary precautions in using a good weld geometry, welding sequence, preheating, interpass temperature, controlled cooling rate, and ultrasonic inspection. It is significant that, in the specimen tested here, the copes were ground smooth, the root pass for the full-penetration weld was located in the back-up bar, the web was welded completely prior to welding of the flanges, cooling rate was controlled, and continuous inspection was utilized.

Additional research is needed to further identify the relative importance of the various factors contributing to the poor performance of some full-penetration splices. Design recommendations should be devised based on this assessment. The influence of axial load and shear on splice behavior should be evaluated.

### **ACKNOWLEDGMENTS**

The funding of this research through a grant from the California Steel Workers Administrative Trust Fund is gratefully acknowledged, as is the administration by the American Institute of Steel Construction. In addition, the donations of some specimens by Western States Steel and The Herrick Corporation substantially contributed to the success of this work. The writers wish to acknowledge participation of H. J. Degenkolb, Roger Ferch, John Fisher, Rudy Hofer, James Marsh, Lowell Napper, and Del Shields as members of an advisory panel. The assistance of Egor Popov is especially appreciated. Additional thanks are extended to Al Collins, welding consultant,

for his valuable comments. The findings and conclusions of this paper are, however, those of the writers alone.

## APPENDIX I. REFERENCES

- Bjorhovde, R. (1987). "Welded splices in heavy wide-flange shapes." *Proc. Nat. Engrg. Conf. and Conf. of Operating Personnel*, New Orleans.
- Blodgett, O. W. (1977). "Why welds crack—How cracks can be prevented." *Publication G230*, The Lincoln Electric Co., Cleveland, Ohio.
- Blodgett, O. W. (1979). "Distortion . . . how to minimize it with sound design practices and controlled welding procedures plus proven methods for straightening distorted members." *Publication G261*, The Lincoln Electric Co., Cleveland, Ohio.
- Bruneau, M., Mahin, S. A., Popov, E. P. (1987). "Ultimate behavior of butt welded splices in heavy rolled steel sections." *EERC Report No. 87-10*, Sep., Earthquake Engineering Research Center, Univ. of California, Berkeley, Calif.
- "Commentary on highly restrained welded connections." (1973). *Engrg. J. Am. Inst. Steel Constr.*, 10(3).
- Doty, W. D. (1987). "Procedures for thermal cutting and welding heavy structural shapes." *Nat. Engrg. Conf. and Conf. of Operating Personnel*, New Orleans, April 29–May 2, 1987, p. 16-1.
- Fisher, J. W., and Pense, A. W. (1987). "Experience with use of heavy W shapes in tension." *Engrg. J. Am. Inst. Steel Constr.*, 24(2), 63–77.
- "Fundamentals of welding." (1976). *Welding handbook: Vol. 1*, 7th Ed., American Welding Society, Miami, Fla.
- Kaufmann, E. J., and Stout, R. D. (1983). "The toughness and fatigue strength of welded joints with buried Lamellar tears." *Welding Research—Supplement to the Welding J.*, American Welding Society, Nov., G2(11).
- Mahin, S. A., and Bertero, V. V. (1976). "Problems in establishing and predicting ductility in aseismic design." *Int. Symp. on Earthquake Structural Engineering*, Aug., 613–628.
- Park, R., and Paulay, T. (1975). *Reinforced concrete structures*. John Wiley and Sons, Inc., New York, N. Y.
- Popov, E. P., and Stephen, R. M. (1976). "Tensile capacity of partial penetration welds." *EERC Report No. 70-3*, Oct., Earthquake Engineering Research Center, Univ. of California, Berkeley, Calif.
- Preece, F. R. (1981). "Structural steel in the 80's—Materials, fastening and testing." *The Steel Committee of California*, San Francisco, Calif.
- "Recommended Lateral Force Requirements and Tentative Commentary—1988." (1988). Seismology Committee, Structural Engineers Association of California.
- "Specifications for the design, fabrication and erection of structural steel for buildings with commentary." (1980). *Manual of steel construction*, AISC, Chicago, Ill.
- "Specifications for the design, fabrication and erection of structural steel buildings with commentary: Supplement no. 2." (1989). *Manual of Steel Construction*, AISC, Chicago, Ill.
- Tuchman, J. L. (1986). "Cracks, fractures spur study." *Engrg. News Rec.*, Aug. 21.
- Uniform building code*. (1985). International Conference of Building Officials, Pasadena, Calif.
- Uniform building code*. (1988). International Conference of Building Officials, Pasadena, Calif.
- "Welding manual for heavy wide flange shapes." (1983). Nippon Steel Corp., Sep.
- Yurioka, N., et al. (1983). "Determination of necessary preheating temperature in steel welding." *Welding Research—Supplement to the Welding J.*, American Welding Society, Jun.

## APPENDIX II. NOTATION

*The following symbols are used in this paper:*

- $C$  = seismic numerical coefficient;  
 $I$  = importance factor;  
 $K$  = structural system performance factor (UBC);  
 $K_l$  = stress intensity factor;  
 $M$  = bending moment;  
 $M_y$  = yield moment;  
 $M_p$  = plastic moment;  
 $P$  = axial force;  
 $P_y$  = yield axial force;  
 $R_w$  = structural system performance factor;  
 $S$  = numerical coefficient for site-structure resonance;  
 $t$  = flange thickness;  
 $T$  = fundamental elastic period of vibration of building  
 (for UBC equation only);  
 $w$  = web thickness;  
 $W$  = total dead load (for UBC equation only);  
 $V$  = total lateral force of base shear;  
 $Z$  = numerical coefficient dependent on seismic zone;  
 and  
 $\mu_1^+, \mu_2^-, \mu_2^*, \mu_3^+, \mu_3^*$  = various expression of ductility defined in Fig. 13.